PHYSICAL REVIEW E **73**, 011702 (2006)

Electromigration of microspheres in nematic liquid crystals

I. Dierking,* G. Biddulph, and K. Matthews
School of Physics and Astronomy, University of Manchester, Schuster Building Oxford Road, Manchester M13 9PL, United Kingdom

(Received 9 August 2005; revised manuscript received 7 October 2005; published 4 January 2006)

Application of an electric field to microspheres, dispersed in a nematic liquid crystal host material, causes particle translation along the direction of the average long molecular liquid crystal axis, i.e., the director. We have determined the stability regime of linear particle displacement in the parameter space of electric field amplitude and frequency for various applied electric wave forms and demonstrate a linear relationship between microsphere velocity and applied electric field amplitude. For increasing frequency the particle velocity exhibits a maximum before motion slowly vanishes. Addition of a small amount of an ionic dopant is shown to largely increase the stability region of linear microsphere motion, with particle velocities increasing until saturation is observed for increasing ion dopant concentration. It is presumed that the particle velocity is related to the surface charges adsorbed on the dispersed particles. Also the dynamics of occasionally observed two- and three-particle clusters is discussed.

DOI: 10.1103/PhysRevE.73.011702 PACS number(s): 61.30.−v, 82.45.−h, 45.50.−j

I. INTRODUCTION

The study of the motion of particles, dispersed in a fluid medium while subjected to an electric field, has been a long-standing topic in science. The phenomenon, named electrophoresis, covers the rotational as well as the translation motion of particles and is used in a wide variety of applications ranging from analytical chemistry and biology [1] all the way to display technologies [2]. First investigations go back to the 19th century when Weiler reported on a field-induced translation of chininsulfate particles in turpentine-oil [3], and Quincke discussed the rotation of solid particles in a liquid subjected to constant electric fields [4]. It took almost a century to describe this rotation theoretically [5] and was later linked to bifurcation behavior [6]. Nevertheless, electrophoresis is mainly discussed in relation to translational particle motion in isotropic liquids. For small amplitudes this motion proceeds with a velocity proportional to the electric field, $\mathbf{v}=\mu\mathbf{E}$, where μ is the electrophoretic mobility. For spherical particles the motion is directed *parallel* to the direction of the applied electric field. Considerable theoretical work has been reported for static [7] and alternating [8] electric fields, spheroidal [9] and slender particles [10,11], as well as particles with a nonuniform charge distribution [12,13]. It was pointed out that in the case of nonspherical particles the velocity vector does not need to be parallel to the applied electric field vector [7]. Electric field induced particle motion in an isotropic matrix seems to be largely understood.

It is thus surprising that only very little work in this direction has been reported for liquid crystals, because the motion of microspheres can lead towards techniques of microrheology [14–16], especially for the determination of the viscosity anisotropy on a microscopic scale [17]. This would be a true advancement in liquid crystal viscosity determination over the classic macroscopic measurements of Kneppe and Schneider [18] more than two decades ago.

To date, experimental reports of micron-sized particles in liquid crystals often concentrate on the large volume fraction regime [19,20], while studies of individual microsphere migration in thermotropic liquid crystals have so far been largely qualitative. Circular motion along macroscopic trajectories was reported for the isotropic and cholesteric (N^*) phases [21], while linear motion along the layer plane was observed for the smectic phases [16,21]. For such translations a certain threshold voltage must be exceeded when applying symmetric fields, while it has been reported that asymmetric fields lead to threshold-less motion [21]. For all cases it is important to notice that the macroscopic particle motion in liquid crystals takes place in a plane perpendicular to the applied electric field direction. This is in contrast to the parallel motion discussed for the electrophoresis of spherical particles in isotropic liquids.

The dynamic behavior of microspheres in anisotropic fluids, subjected to electric fields, is obviously rather complicated. It displays a strikingly rich variety of particle motions: rotation, translation, and irregular movement, all depending on the investigated liquid crystal phase, the applied external conditions and the aggregation status of the particles. To our knowledge there is no theoretical model available to describe such behavior. Even the cause of translational motion of spherical particles in liquid crystals perpendicular to the applied field direction seems to be largely unclear, although it has been proposed that this may be linked to a varied local charge distribution around rotating particles [16]. In this paper we will concentrate on the translational motion of uniform microspheres in the simplest of all liquid crystal phases: the nematic phase under unidirectional boundary conditions, exhibiting solely orientational order.

II. EXPERIMENT

The liquid crystal employed in this investigation was the commercially available and well-known room-temperature

---

*Author to whom correspondence should be addressed. Electronic address: ingo.dierking@manchester.ac.uk

1539-3755/2006/73(1)/011702(6)/$23.00

nematic mixture E7 from Merck. Monodisperse spherical glass particles of diameter $D=4$ μm were added to the liquid crystal at very small concentration. The SiO_x spheres were not treated for any special surface alignment conditions. As the employed liquid crystal mixture orients planar on plain glass, we presume that also in the case of the microspheres such an orientation is retained. Nevertheless, we unfortunately do not have conclusive evidence for any preferred anchoring conditions, as characteristic hyperbolic hedgehog [22], Saturn ring [23,24] or boojum defects [22], which provide a clue towards planar or homeotropic anchoring on the particles, could not be resolved by optical microscopy. The measurements presented below were obtained for single particles unless otherwise noted. Care was taken to only observe particles, which were separated from others by a distance as far as possible in order to minimize any influences from the flow field created by the motion of other particles. For the second part of the studies, concerning the influence of an ionic dopant, the following rod shaped, but nonmesogenic molecule (ASE2, Merck) was additionally added at varying concentration.

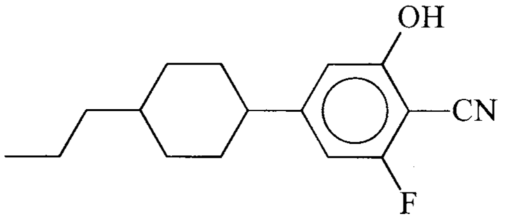

The resulting mixtures were introduced into commercial Hele-Shaw cells (E.H.C., Japan) of cell gap $d=10$ μm by capillary action. The bounding glass plates are coated with an optically transparent ITO layer to act as electrodes and a thin, unidirectionally rubbed polyimide layer to promote planar boundary conditions for the liquid crystal. The resulting sample geometry is schematically summarized in Fig. 1. (Note that the size of the liquid crystal molecules is largely exaggerated.) From the employed geometry, i.e., $D=4$ μm particles in $d=10$ μm cells, it is clear that any classical electrophoretic behavior with particle motion along the applied electric field direction is not resolvable in our experiments.

Electric fields were applied at varying wave form, amplitude and frequency by a function generator (TTi TG1010) in combination with an in house built high voltage amplifier. Particle motion was monitored at room temperature via a polarizing microscope (Nikon Optiphot-pol) equipped with a digital camera (JVC KY-F1030). Images were recorded at a spatial resolution of 1280×960 pixels, corresponding to an image size of 520×390 μm^2, at a maximum time resolution of 1 s. Subsequent image analysis was carried out with software IMAGETOOL3.0, developed at the University of Texas Health Science Center, San Antonio.

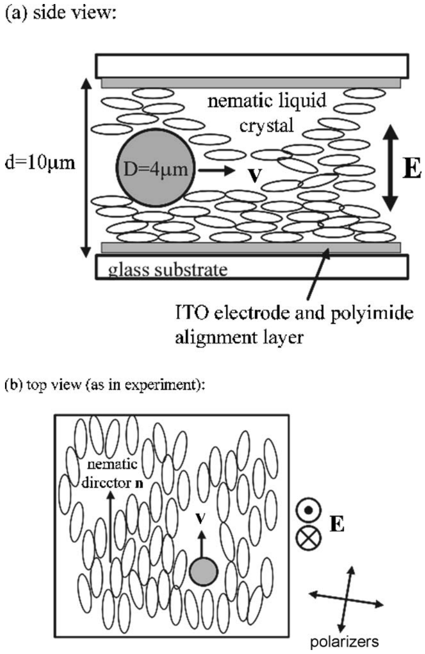

FIG. 1. Schematic illustration of the experimental conditions. (a) Side view of the employed Hele-Shaw cell with cell gap $d=10$ μm. At zero electric field the nematic director **n** is approximately parallel to the bounding substrates. Particle motion is observed in the plane perpendicular to the direction of the applied electric field. (b) Top view of the cell as observed in the polarized microscopic experiments. At zero applied field the director **n** is uniformly oriented along a preferred direction. Particle motion is observed parallel to this direction and perpendicular to the applied ac electric field direction.

III. RESULTS AND DISCUSSION

Particles can be moved through a fluid liquid crystal matrix at relative ease. It has been shown that microspheres can be trapped at defects or the interface between the isotropic and the liquid crystal phase and be dragged along as defects or interfaces move [25–27]. Similarly, particles can be collected in the liquid crystal state through loop defects. This is demonstrated in the time series of Fig. 2, where a defect loop collapses, bringing together a number of microspheres to form an aggregate before annihilation of the defect. The force exerted on particles by a moving line defect is thus strong enough to cause particle motion. It is interesting to note the reaction of such an aggregate of microspheres to a subsequently applied electric field, which is depicted in the time series of Fig. 3. The particles repel each other, indicating field induced surface charges of equal polarity, which may well be the cause for the electrotranslational motion of spheres in liquid crystals.

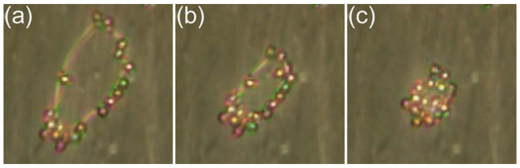

FIG. 2. (Color online) Exemplary time series of the collection of microspheres towards a cluster of particles by a collapsing defect loop in the nematic phase at zero applied electric field. (a) $t-t_0=6$ s, (b) $t-t_0=3$ s, and (c) $t-t_0=0$ s. The value of $t-t_0$ describes the time to defect annihilation. The displayed image size is 120×120 μm^2.

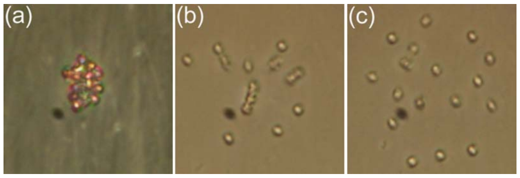

FIG. 3. (Color online) Exemplary time series showing the repulsion of particles from a cluster during electric field application at amplitude $E=8\ \text{V}\ \mu\text{m}^{-1}$ and frequency $f=13$ Hz. (a) $t=0$ s, (b) $t=2$ s, and (c) $t=4$ s. The displayed image size is $120\times 120\ \mu\text{m}^2$.

When applying an electric field to a nematic liquid crystal doped with single spherical particles, the latter can be observed to move after a certain threshold electric field is passed. The motion of individual particles is direct along the director **n** and perpendicular to the electric field. Within a certain regime of electric field amplitude and frequency, the distance L that a particle is translated is observed to increase linearly with time, as depicted in Fig. 4. This allows an easy determination of the microsphere's velocity **v**, which depends on the applied electric field wave form. At equivalent conditions of $E=8\ \text{V}\ \mu\text{m}^{-1}$ and $f=13$ Hz, particle velocities are rather similar for triangular and sinusoidal fields, $v=(3.0\pm0.2)\ \mu\text{m s}^{-1}$ and $v=(3.4\pm0.2)\ \mu\text{m s}^{-1}$, respectively, but increase to $v=(7.8\pm0.2)\ \mu\text{m s}^{-1}$ for applied square wave fields. Although not quite realized on a quantitative basis, this indicates that the important parameter is the effective voltage applied to the system.

It is also worthwhile to point out that the particle motion is in fact directed, which may not be readily expected, due to the fact that the director is actually a pseudovector with the property $\mathbf{n}=-\mathbf{n}$. For symmetry reasons, the latter implies an equal number of particles moving in $+\mathbf{x}$ as in $-\mathbf{x}$ direction. Nevertheless, this is not observed experimentally and we attribute the symmetry breaking to a directed Freedericksz transition caused by a slight director pretilt angle at the bounding substrates. Only on very rare occasions did we observe particle translation in opposite directions, and only once, out of several hundred of measurement series, a reversal in direction during the measurement. For statistical reasons such data was omitted from the discussion below.

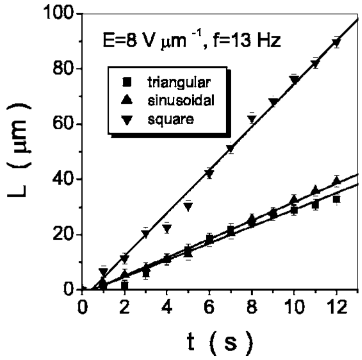

FIG. 4. Displacement L along the direction of the director of a single microsphere as a function of time for different applied electric wave forms, triangular (squares), sinusoidal (up triangles), and square wave (down triangles), at electric field amplitude $E=8\ \text{V}\ \mu\text{m}^{-1}$ and frequency $f=13$ Hz. The motion is linear, allowing the determination of the particle velocity from the slope of the curves. The latter increases as $v_{\text{triangle}}<v_{\text{sinusoidal}}<v_{\text{square}}$ in approximate relation to the effective voltages applied.

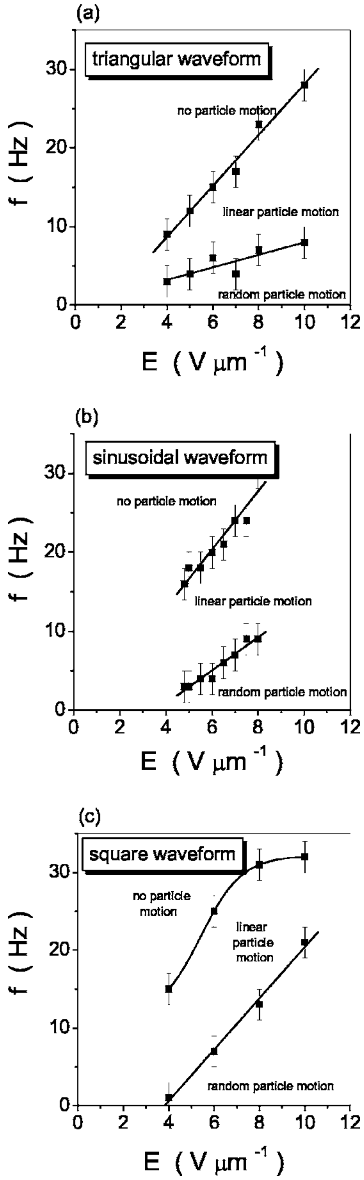

FIG. 5. Stability regions in amplitude-frequency space for the different types of translational motion observed for a single dispersed microsphere for (a) triangular, (b) sinusoidal, and (c) square-wave field application.

Figure 5 illustrates the parameter spaces for the different types of particle motion observed for varying electric field amplitude E and frequency f for (a) triangular, (b) sinusoidal, and (c) square wave fields. Below a certain threshold amplitude no particle migration is observed at all. Increasing the field amplitude at low frequencies leads to irregular motion of the dispersed microspheres. Only within a regime of moderate electric field amplitudes and frequency is linear particle translation observed. Motion ceases for further increasing frequencies. In general, the frequency for linear particle motion at both limits of the regime increases with increasing electric field amplitude for all wave forms applied. At large

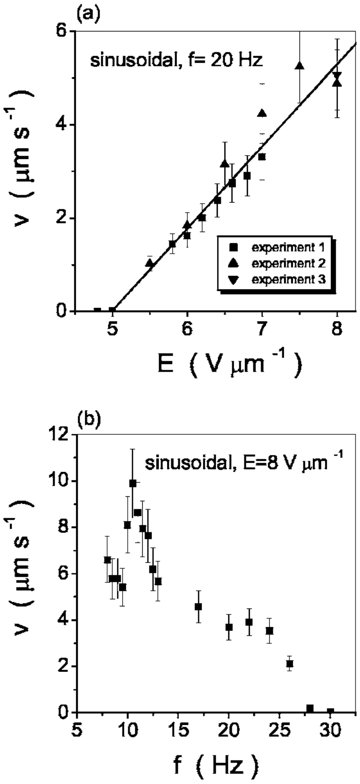

FIG. 6. (a) Velocity dependence of a single microsphere as a function of applied sinusoidal field amplitude E. The particle velocity v increases linearly above a threshold field of $E_{\mathrm{th}}=5\ \mathrm{V}\ \mu\mathrm{m}^{-1}$, as depicted for several independent measurement series. (b) The frequency dependence of the particle velocity exhibits a maximum and microsphere motion ceases for increasing frequency of the applied electric field. Note that an equivalent behavior is also observed for other applied wave forms, with the velocity maximum shifted towards higher frequencies for the square wave field.

amplitudes ($E > 10\ \mathrm{V}\ \mu\mathrm{m}^{-1}$) electroconvection sets in, which obviously marks a further regime, which was not studied within the scope of this investigation.

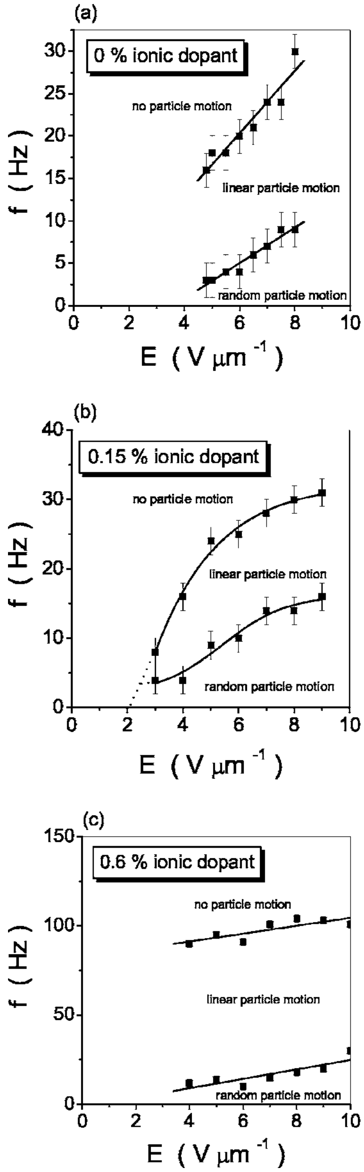

FIG. 7. Stability regions in amplitude-frequency space for the different types of translational motion observed for the dispersed microspheres at increasing concentration of an ionic dopant, (a) pure E7, (b) 0.15%, and (c) 0.6% of ASE2 by weight. The stability regime of linear particle motion is greatly enhanced by adding small amounts of an ionic molecule.

In Fig. 6 the dependence of the microsphere velocity on applied electric field parameters is exemplary depicted for the sinusoidal wave form in the stability regime of constant particle velocity. At constant frequency the velocity increases linearly with applied electric field amplitude above a threshold field E_{th} as shown in Fig. 6(a) for several independent experiments. This threshold field ($E_{\mathrm{th}}=5\ \mathrm{V}\ \mu\mathrm{m}^{-1}$) is much larger than the threshold field of the director reorientation of the neat E7 mixture. Indeed, the nematic, electric Freedericksz transition exhibits a threshold voltage of $V_{\mathrm{th}}^{F}=1\ \mathrm{V}$, which is independent of cell gap d, i.e., the threshold field for the nematic liquid crystal Freedericksz transition changes according to cell gap. In our case $d=10\ \mu\mathrm{m}$, thus implying a Freedericksz threshold field of approximately $E_{\mathrm{th}}^{F}=0.1\ \mathrm{V}\ \mu\mathrm{m}^{-1}$. For increasing frequency at constant field amplitude above the threshold, the particle velocity exhibits a maximum, slowly tending towards zero as the frequency is further increased [Fig. 6(b)]. This general behavior is observed for all applied wave forms, although with varying slope dv/dE and the frequency of maximum velocity shifted towards larger values for the square wave fields.

In order to gain a first general understanding of the nature of the particle translation process, we investigated the dependence of microsphere migration under applied electric fields on the contents of ions present within the liquid crystal. Data shown below was obtained for sinusoidal field application. The commercial LC was deliberately doped with an ionic compound of quasi-rod-like shape (see above). Figure 7 shows the parameter regimes of irregular, linear and ceasing particle motion at sinusoidal field application for different ionic dopant concentrations, (a) the pure LC, (b) $c_{\mathrm{ion}}=0.15\%$ by weight, and (c) $c_{\mathrm{ion}}=0.6\%$ by weight. The general, qualitative behavior is equivalent for all samples, but a clear expansion of the linear translational motion regime is

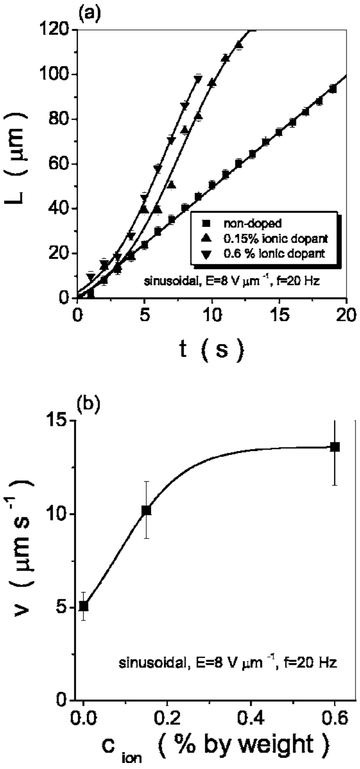

FIG. 8. (a) Particle displacement L as a function of time for different ionic dopant concentrations. At short times $t < 5$ s microsphere motion appears to be nonlinear for the doped samples. (b) For the linear regime, $t > 5$ s, the particle velocity increases with increasing ionic dopant concentration and approaches saturation at approximately $c_{\text{ion}} = 0.4\%$ by weight.

observed for increasing ionic dopant concentration. This may be caused by an increased adsorption of ions at the microsphere surfaces, presuming that a surface charge on the particles is the cause for the translational motion.

Every liquid crystal contains ionic impurities. However, commercial liquid crystals like E7 are extensively purified of ionic contamination. It can thus be assumed that ion adsorption at the particle surfaces is unsaturated at a constant level for the neat E7 mixture. This can be inferred from the basically constant stability regimes for linear particle motion of Fig. 5. Addition of an ionic dopant leads to increasing particle surface charges until saturation and to an increase in the stability regime for increasing ion concentration (Fig. 7).

For added ions the particle displacement becomes slightly nonlinear at the early times of electric field application, $t < 5$ s [Fig. 8(a)]. This behavior is not understood presently, as ion adsorption should take place at relatively short time scales. The observed behavior rather indicates an electric field induced ion adsorption process at the microsphere surfaces before an increased particle velocity is obtained. Nevertheless, the particle velocity is observed to increase with increasing ionic dopant concentration until saturation [Fig. 8(b)]. We believed that the saturation velocity is related to the saturation of charges at the surface of each dispersed microsphere.

In rare events, two or three microspheres actually stick together and perform a combined motion as a cluster of particles. Considering the generally observed repulsion of particles, as demonstrated in Fig. 3, this behavior must be regarded as exceptional. Nevertheless, it is very interesting, also with respect to the nematic defects which are formed around inclusions, to experimentally investigate the dynamics of such aggregates. Why are such aggregates even formed? One reason could be the attractive forces between particle inclusions mediated via nematic director field defects in the close spatial vicinity of dispersed particles [22–24,28]. If such attractive forces are larger than electrostatic repulsion due to surface charges, aggregates may be formed and occasionally be stable under applied electric field conditions.

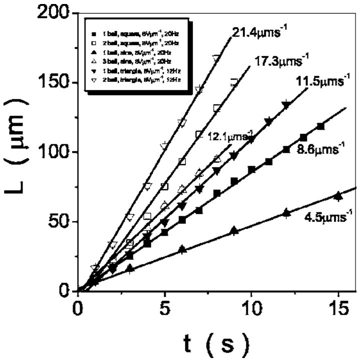

FIG. 9. On few occasions microspheres can be observed to stick together and translate as a cluster of two or three particles. In this case the cluster velocity is found to be approximately twice or three times as large as that of individual particles, respectively. This observation is independent of applied electric wave form: (■) and (□) at applied square wave voltage for a single and a two sphere system, (▲) and (△) at a sinusoidal wave form applied to a single and a three sphere system, and (▼) and (▽) at a triangular wave form applied to a one and two sphere system.

We have inferred above that the particle velocity v is proportional to the surface charge ρ of a particle. This surface charge ρ increases with the surface area A of a sphere. Thus the particle's velocity should be proportional to its squared radius, $v \sim r^2$, neglecting any viscous drag. In the case of the two- or three-particle clusters, one can make the rough approximation that the total surface area is about equal to the sum of the areas of the individual particles of the cluster, i.e., $A_{\text{total}} \approx \Sigma A_{\text{spheres}}$ for small numbers of spheres. Thus, the cluster velocity should in first approximation increase with the number of aggregated particles (in the crude limit of only very few spheres and again neglecting changes in viscous drag). This is demonstrated in Fig. 9 for the neat liquid crystal matrix (no ionic doping) for three individual events. For a square wave electric field, the velocity of a two-particle cluster ($v = 17.3\ \mu\text{m s}^{-1}$, open squares) is found to be twice as large as that of a single microsphere ($v = 8.6\ \mu\text{m s}^{-1}$, closed squares) under equivalent experimental conditions. The same behavior is observed in the case of an applied triangular field, $v = 11.5\ \mu\text{m s}^{-1}$ for the single microsphere (closed down triangles) and $v = 21.4\ \mu\text{m s}^{-1}$ for the two-particle cluster (open down triangles). Finally, for an applied sinusoidal field, the velocity of a three-particle cluster was observed to be approximately three times larger than that of a single microsphere, $12.1\ \mu\text{m s}^{-1}$ (open up triangles) compared to 4.5 μms^{-1} (closed up triangles), respectively. The fact that the measured aggregate velocities increase somewhat less than expected can most likely be attributed to an increase in viscous drag force. The latter has largely been neglected in our discussion, because it is not accessible from our experiments. But it should be noted that viscous drag does of course play a role in the dynamics of particle motion in liquid crystals, depending on particle shape, viscosity, and director configuration around the particles. This has been pointed out in theoretical studies [29–31] as well as in a recent experimental investigation [32].

IV. CONCLUSIONS

The study of the dynamics of micron-sized particle migration in a fluid environment offers interesting possibilities for the determination of viscosities on a local, nonmacroscopic scale (microrheology). This is of special importance for anisotropic fluids like liquid crystals, because of their intrinsic directional dependence of the local viscosity. We have provided a first quantitative characterization of model particle migration in a thermotopic liquid crystal, employing the simplest of anisotropic fluids available, the nematic phase. Within the linear stability regime microsphere motion is directed along the nematic director, and proportional to the applied field amplitude above an electric threshold value. For increasing frequency particle motion ceases. The regime of linear migration as well as the particle velocity can be increased by the addition of a small amount of an ionic dopant. The velocity of two- and three-particle microsphere clusters is roughly proportional to the number of particles at otherwise equivalent conditions. The results indicate that surface charges adsorbed on the particles may be the driving force for microsphere migration.

ACKNOWLEDGMENT

The authors would like to thank Merck, Darmstadt, for providing the liquid crystal host material E7 and the ionic dopant ASE2.

[1] D. M. Hawcroft, *Electrophoresis: The Basics* (Oxford University Press, Oxford, 1997).
[2] S.-T. Wu and D.-K. Yang, *Reflective Liquid Crystal Displays* (Wiley, Chichester, 2001), Chap. 1.
[3] W. Weiler, Z. Phys. Chem. Unterricht, **6**, 194 (1893).
[4] G. Quincke, Ann. Phys. Chem. **11**, 27 (1896).
[5] T. B. Jones, IEEE Trans. Ind. Appl. **1A-20**, 845 (1984).
[6] I. Turcu, J. Phys. A **20**, 3301 (1987).
[7] R. W. O'Brien and L. R. White, J. Chem. Soc., Faraday Trans. 1 **74**, 1607 (1978).
[8] C. S. Mangelsdorf and L. R. White, J. Chem. Soc., Faraday Trans. **88**, 3567 (1992).
[9] B. J. Yoon and S. Kim, J. Colloid Interface Sci. **128**, 275 (1988).
[10] Y. Solomentsev and J. L. Anderson, J. Fluid Mech. **279**, 197 (1994).
[11] D. Long and A. Ajdari, Phys. Rev. Lett. **81**, 1529 (1998).
[12] B. J. Yoon, J. Colloid Interface Sci. **142**, 575 (1991).
[13] Y. E. Solomentsev, Y. Pawar, and J. L. Anderson, J. Colloid Interface Sci. **158**, 1 (1993).
[14] D. Mizuno, Y. Kimura, and R. Hayakawa, Phys. Rev. Lett. **87**, 088104 (2001).
[15] D. Mizuno, Y. Kimura, and R. Hayakawa, Phys. Rev. E **70**, 011509 (2004).
[16] G. Liao, I. I. Smalyukh, J. R. Kelly, O. D. Lavrentovich, and A. Jakli, electronic-Liquid Crystal Communications, 2005. (http://www.e-lc.org/docs/2005_02_25_10_57_49), accessed June 2005; G. Liao, I. I. Smalyukh, J. R. Kelly, O. D. Lavrentovich, and A. Jakli, Phys. Rev. E **72**, 031704 (2005).
[17] H. F. Gleeson, T. Wood, and M. R. Dickinson (unpublished).
[18] H. Kneppe and F. Schneider, Mol. Cryst. Liq. Cryst. **65**, 23 (1981).
[19] S. P. Meeker, W. C. K. Poon, J. Crain, and E. M. Terentjev, Phys. Rev. E **61**, R6083 (2000).
[20] V. J. Anderson, E. M. Terentjev, S. P. Meeker, J. Crain, and W. C. K. Poon, Eur. Phys. J. E **4**, 11 (2001); V. J. Anderson and E. M. Terentjev, *ibid.* **4**, 21 (2001).
[21] T. Togo, K. Nakayama, M. Ozaki, and K. Yoshino, Jpn. J. Appl. Phys., Part 2 **36**, L1520 (1997); K. Nakayama, M. Ozaki, and K. Yoshino, Mol. Cryst. Liq. Cryst. Sci. Technol., Sect. A **329**, 129 (1999).
[22] P. Poulin and D. A. Weitz, Phys. Rev. E **57**, 626 (1998).
[23] O. Mondain-Monval, J. C. Dedieu, T. Gulik-Krzywicki, and P. Poulin, Eur. Phys. J. B **12**, 167 (1999).
[24] Y. Gu and N. L. Abbott, Phys. Rev. Lett. **85**, 4719 (2000).
[25] D. Voloschenko, O. P. Pishnyak, S. V. Shiyanovskii, and O. D. Lavrentovich, Phys. Rev. E **65**, 060701(R) (2002).
[26] J. L. West, A. Glushchenko, G. Liao, Y. Reznikov, D. Andrienko, and M. P. Allen, Phys. Rev. E **66**, 012702 (2002).
[27] J. L. West, K. Zhang, A. V. Glushchenko, Y. Reznikov, and D. Andrienko, Mol. Cryst. Liq. Cryst. **422**, 73 (2004).
[28] H. Stark, Phys. Rep. **351**, 387 (2001).
[29] R. W. Ruhwandl and E. M. Terentjev, Phys. Rev. E **54**, 5204 (1996).
[30] H. Stark and D. Ventzki, Phys. Rev. E **64**, 031711 (2001).
[31] J. Fukuda, H. Stark, M. Yoneya, and H. Yokoyama, J. Phys.: Condens. Matter **16**, S1957 (2004).
[32] J. C. Loudet, P. Hanusse, and P. Poulin, Science **306**, 1525 (2004).